

Analytical Methods

Accepted Manuscript



This is an *Accepted Manuscript*, which has been through the Royal Society of Chemistry peer review process and has been accepted for publication.

Accepted Manuscripts are published online shortly after acceptance, before technical editing, formatting and proof reading. Using this free service, authors can make their results available to the community, in citable form, before we publish the edited article. We will replace this *Accepted Manuscript* with the edited and formatted *Advance Article* as soon as it is available.

You can find more information about *Accepted Manuscripts* in the [Information for Authors](#).

Please note that technical editing may introduce minor changes to the text and/or graphics, which may alter content. The journal's standard [Terms & Conditions](#) and the [Ethical guidelines](#) still apply. In no event shall the Royal Society of Chemistry be held responsible for any errors or omissions in this *Accepted Manuscript* or any consequences arising from the use of any information it contains.

Fragmentation patterns of five types of phospholipids by ultra-high-performance liquid chromatography electrospray ionization quadrupole time-of-flight tandem mass spectrometry

Juanjuan Pi, Xia Wu, Yifan Feng*

Fragmentation patterns of phospholipids have been thoroughly studied in previous researches. Actually, most researches only concentrated on these patterns of several phospholipids in single ion mode (positive or negative ion mode) which have not provided a systematic summarization of more phospholipids. Since phospholipidomics studies need high throughput screening of target phospholipids, the necessity for rapid identification schemes of them becomes obvious. Fragmentation patterns of five major kinds of phospholipids including phosphatidylcholine (PC), phosphatidylethanolamine (PE), phosphatidylserine (PS), phosphatidylinositol (PI) and sphingomyelins (SM) in different ion modes at several elevated collision energies (10-50 eV) have been studied by ultra-high-performance liquid chromatography electrospray ionization quadrupole time-of-flight tandem mass spectrometry (UHPLC/ESI-Q-TOFMS). The different characteristic ions of phospholipids in ESI (+/-) modes, three possible patterns ($[\text{RC}=\text{O}]^+$, $[\text{RCOO}]^-$, and neutral ion $\text{R}'\text{CH}=\text{CO}$) of fatty acyl chains in ESI (+/-) modes, and the change of abundance ratios of the *sn*-1/*sn*-2 carboxylate anion of phospholipids at different collision energies used to fast identify the positions of fatty acyl chains of phospholipids were revealed. Fragmentation patterns of five major types of phospholipids were systematically summarized. This summary provides reference tools for rapid identification of phospholipids and the opportunity to obtain complementary and more comprehensive results in future phospholipidomics studies.

1 Introduction

Phospholipids were often classified in two kinds of glycerophospholipids which exist widely in lives and sphingomyelins (SM). The glycerophospholipids, naming involves a stereo-specific numbering (*sn*), were consisted of a glycerol backbone with alkylation or acylation at the *sn*-1 and/or *sn*-2 positions and a phosphate ester at *sn*-3 position.¹ The various fatty acyl substituents linked in *sn*-1 and/or *sn*-2 carbons enrich the molecular diversity of each kind of

Central laboratory, Guangdong Pharmaceutical University, No. 280, East Rd of outer ring in College Station, Panyu District, Guangzhou City, Guangdong Province, China. E-mail: tfengyf@163.com

1
2
3 glycerophospholipids. The *sn*-3 carbon participates in phosphodiester linkage to different polar
4 head groups, which tentatively classified glycerophospholipids into five major types of
5 phosphatidylcholine (PC), phosphatidylethanolamine (PE), phosphatidylserine (PS),
6 phosphatidylinositol (PI) and phosphatidylglycerol (PG). Phospholipids play important roles in
7 components of cell membranes, membrane fusion, signal transduction and receptor ligands.²⁻⁷
8 Furthermore, recent evidences continue to accrue, implicating that the pathogenesis of numerous
9 human chronic diseases, such as diabetes and obesity maybe caused by metabolism disorder of
10 phospholipids.⁸⁻¹¹ Thus more and more interests have been attracted in the research of
11 phospholipids such as phospholipidomics.¹²⁻¹⁴ It could be a challenging task to analyze
12 phospholipids, since they exist largely in cells or lives as a mixture of molecules with similar
13 structures, wide concentration range and different polarities. Before the popular use of mass
14 spectrometry (MS), thin layer chromatography and gas chromatography were the main analytical
15 methods, which could be used to detect a molecule of a specific class or with a specific fatty acyl
16 chain merely, while not be applied to identify all molecules in a phospholipid mixture.¹⁵⁻¹⁸ The
17 new possibilities in the researches of phospholipids, especially fragmentation patterns which could
18 identify the molecular structure, have been opened by the development of high resolution mass
19 spectrometry (such as Q-TOFMS).¹⁹ Erlend Hvattum, etc, have discussed fragmentation pathway
20 of phosphatidylserine in negative ESI mode, and Yan Xiaojun, etc, have roughly summarized the
21 characteristic daughter ions of glycerophospholipids in negative ESI mode.^{20,21} However, these
22 researches of fragmentation patterns have concentrated on several kinds of phospholipids or single
23 ion mode (positive or negative ion mode) merely,^{20,21} and the common patterns of most
24 phospholipids in all ion modes were not summarized systematically, necessary for rapid
25 identification of target phospholipids in high throughput screening especially phospholipidomics
26 studies.
27
28
29
30
31
32
33
34
35
36
37

38
39 Herein, UHPLC/ESI-Q-TOFMS was utilized to analyze mixed standards of five kinds of
40 phospholipid compositions. The fragmentation patterns of five major types of phospholipids (PE,
41 PI, PC, PS and SM) were studied systematically in different ion modes at several elevated
42 collision energies (10-50 eV). Combining with our previous researches,^{22,23} all these
43 fragmentation patterns were summarized, containing different characteristic ions of phospholipids
44 in different ion modes, three patterns ($[\text{RC}=\text{O}]^+$, $[\text{RCOO}]^-$ and $\text{R}'\text{CH}=\text{CO}$) of common fatty acyl
45 chain ions of glycerophospholipids in different ion modes, and the variation trend of ratios of the
46 *sn*-1/*sn*-2 carboxylate ion in ESI (-) mode at different collision energies (10-50 eV), which could
47 be used to rapid identify the possible phospholipids according to their MS and MS/MS
48 information.
49
50
51
52
53
54
55
56
57

58 2 Experimental

59
60

2.1 Chemicals and reagents

Acetonitrile, methanol and isopropanol of HPLC grade were obtained from Merck (Germany), acetic acid (HPLC-grade) from Aladdin Technologies and leucine-enkephalin from Sigma-Aldrich (USA). Chloroform, hydrochloric acid and ammonium acetate (analytical reagent) were purchased from Fuyu speciality chemical Co. Ltd (China). Doubly distilled water provided by Watson's Food & Beverage (China) was used as the solvent throughout the experiments. Standards PE (18:0/20:4,5Z,8Z,11Z,14Z), PI (18:0/20:4,5Z,8Z,11Z,14Z), PS (16:0/18:1,9Z), PC (18:0/18:2,6Z,9Z) and SM (d18:1/18:0) were purchased from Avanti Polar Lipids Inc (USA).

2.2 Preparation of the standards

All the standards were prepared as the 5 mg/mL mother liquor by chloroform separately. 10 μ l mother liquors were drawn and mixed in a 5 ml volumetric flask, and the mixture was a constant-volume processed by methanol.

2.3 UHPLC condition

ACQUITY UHPLC/Q-TOFMS system (Waters, USA) equipped with binary Pump, vacuum degasser and autosampler was controlled with MassLynxTM (V4.1) software. Separation was performed at 50 °C on an ACQUITY UHPLC BEH C18 column (2.1 mm \times 50 mm, 1.7 μ m; Waters). The mobile phases were consisted of water containing 10 mM ammonium acetate and 0.1% acetic acid (A), and 50% acetonitrile-isopropanol (V/V) containing 10 mM ammonium acetate and 0.1% acetic acid (B) with flow rate of 0.3 mL/min. A gradient elution program was set as follows: 60–81.4% B at 0–4 min, 81.4–90% B at 4–20 min.²²

2.4 MS condition

ACQUITY UHPLC/Q-TOFMS system was equipped with an ESI ion source operating in positive ion mode (ESI+) and negative ion mode (ESI-). The spectra were acquired in the range of m/z 420-950 for full scan time MS analysis and m/z 80-800 for MS/MS analysis. High-purity nitrogen (N₂) was used as the desolvation gas at a flow rate of 500 L/h and ultrahigh-purity helium (He) as the collision gas. The flow rate of cone gas (N₂) was 50 L/h. The desolvation and source temperature were 350 °C and 120 °C, respectively. The cone voltage was 3000 V, capillary voltage 2300 V for ESI (+/-) and sample cone 30V. The MS/MS analysis was performed using variable collision energies (10, 20, 30, 40 and 50 eV). To ensure accuracy during the MS analysis, the acquired data was corrected via an external reference (Lock-SprayTM) consisted of leucine-enkephalin with [M+H]⁺ = 556.2771 in ESI (+) and [M-H]⁻ = 554.2615 in ESI (-). All data collected in ESI (+) and ESI (-) modes was acquired using MassLynxTM (V4.1) software system.

3 Results and discussion

3.1 The fragmentation regularities of PE and PI

The fragmentation patterns of standards PE (18:0/20:4) and PI (18:0/20:4) at different MS² collision energies (10-50 eV) were investigated in ESI (+) mode, shown in **Fig. 1(a)** and **Fig. 2(a)**. At the collision energies of 10 and 20 eV, PE (18:0/20:4) predominantly formed the ions at m/z 768 $[M+H]^+$ and further lost the polar head group to produce the ions at m/z 627 $[M+H-141]^+$. The ion $[M+H-141]^+$ was considered as the characteristic ion of PE in ESI (+) mode.²⁴ The ions at m/z 341 $[M+H-141-C_{18}H_{33}CHCO]^+$ arised from the precursor ions at m/z 627 by a loss of a neutral ion ($C_{18}H_{33}CHCO$) when the collision energies exceed 30 eV. Synchronously, the minor intensity ions at m/z 482 $[M+H-C_{18}H_{33}CHCO]^+$ were detected. In the fragmentation of standard PI (18:0/20:4), the molecular ions at m/z 887 $[M+H]^+$ were formed. Then the molecular ions could produce the ions at m/z 627 $[M+H-H_2PO_4CH(CH(OH))_5]^+$ after losing the phosphate head groups, and further formed the daughter ions at m/z 341 $[627-C_{18}H_{33}CHCO]^+$ following the cleavage of the *sn*-2 ester bond. The fragmentation pathways of PE and PI under ESI (+) were shown in **Fig. 3(a)** and **Fig. 4(a)**.

Fig. 1

Fig. 2

Fig. 3

Fig. 4

In ESI (-) mode, daughter ions at m/z 303 $[R_2COO]^-$, 259 $[R_2COO^-CO_2]^-$, 283 $[R_1COO]^-$, 480 $[M-H-C_{18}H_{33}CHC=O]^-$, characteristic ions at m/z 140 $[C_2H_7O_4NP]^-$ and m/z 196 $[C_5H_{11}O_5NP]^-$ were formed, besides the molecular ions at m/z 766 $[M-H]^-$ of PE (18:0/20:4).²¹ In the fragmentation of PI (18:0/20:4), the molecular ions at m/z 885 $[M-H]^-$ produced the daughter ions at m/z 581 $[M-H-R_2COOH]^-$, m/z 303 $[R_2COO]^-$, m/z 283 $[R_1COO]^-$ and m/z 241 $[C_6H_{10}O_8P]^-$ by the cleavages of ester bonds and polar head group. Then the daughter ions produced ions at m/z 419 $[581-C_6H_{10}O_5]^-$, m/z 223 $[241-H_2O]^-$, m/z 297 $[C_9H_{14}O_9P]^-$ and m/z 153 $[C_3H_6O_5P]^-$ after the further fragmentation. Among them, the ion at m/z 241 $[C_6H_{10}O_8P]^-$ was the characteristic ion of PI, which could be used to distinguish the PI in the biological samples or pharmaceutical products, and the ion at m/z 153 $[C_3H_6O_5P]^-$ was the characteristic ion of all the glycerophospholipids. Their fragmentation pathways were shown in **Fig. 3(b)** and **Fig. 4(b)**. Interestingly, as shown in **Fig. 1(b)** and **Fig. 2(b)**, the *sn*-1/*sn*-2 carboxylate anions of PE (18:0/20:4) and PI (18:0/20:4) at different collision energies were similar in the abundance ratios.^{25,26} The $[R_2COO]^-$ signal was higher than $[R_1COO]^-$ (*sn*-1/*sn*-2<1) of PE (18:0/20:4) and PI (18:0/20:4) at collision energies of 20-30 eV,

1
2
3 and lower than $[R_1COO]^-$ ($sn-1/sn-2 > 1$) at collision energies of 40-50 eV. Structurally, PE
4 (18:0/20:4) and PI (18:0/20:4) have the different polar head groups and same hydrophobic fatty
5 acyl chain. Thus, it was considered that the different structure of the polar head groups of PE
6 (18:0/20:4) and PI (18:0/20:4) contributed equally to the ratio of the $sn-1/sn-2$ carboxylate anions.
7
8 The fragmentation of two acyl chains of glycerophospholipids leading to the formation of the $sn-1$
9 and $sn-2$ carboxylate anions was possibly attack of the anionic site of the phosphate group from
10 path a or b, involving a six- or five-membered ring transition states (see **Fig. 5**), respectively.²⁷
11 Apparently, the abundance ratios of the carboxylate anions of PE (18:0/20:4) and PI (18:0/20:4)
12 are depend mainly upon the stability of the cyclic phosphate ester and the steric hindrance of head
13 groups structure.²⁷ The attack of the phosphate anion at C-1 of the glycerol backbone is
14 unfavourable if there is steric hindrance from the phospholipid head group at low collision
15 energies (20-30 eV).²⁸ PE with primary amine and the carbonyl groups formed intramolecular
16 hydrogen bonds, while PI has a group of inositol, restricting the attack from path a at low
17 collision energies.^{20,25,29} When the collision energy increases, it prefers to form the six-membered
18 ring transition state. It was indicated from above that the anionic site of the phosphate groups of
19 PE (18:0/20:4) and PI (18:0/20:4) tended to form the five-membered ring (produced the $sn-2$
20 carboxylate anions at m/z 303 $[R_2COO]^-$) at low collision energies (20-30 eV), and the
21 six-membered ring at high collision energies (40-50 eV) (produced the $sn-1$ carboxylate anions at
22 m/z 283 $[R_1COO]^-$). Therefore, characteristic ions of PE and PI could be used to
23 qualitative identification and the abundance ratio of the $sn-1/sn-2$ carboxylate anions at different
24 collision energies could be used to identify the positions of the two fatty acyl chains (see **Table 1**).
25
26
27
28
29
30
31
32
33
34

35 **Fig. 5**

36
37 **Table 1**

38 3.2 The fragmentation regularities of PC and PS

39
40
41
42 It was easy for PC known as lecithin to form the molecular ions $[M+H]^+$ and adduct molecular
43 ions $[M+Na]^+$ if the mobile phase containing alkalis (Na^+ , etc.) in ESI (+) mode.³⁰ In ESI (+)
44 mode, standard PC (18:0/18:2) formed the ions at m/z 786 $[M+H]^+$ and characteristic ions at m/z
45 184 $[C_5H_{15}O_4NP]^+$.^{31,32} When the collision energies were set at 30, 40 and 50 eV, daughter ions at
46 m/z 603 $[M-HPO_4CH_2CH_2N(CH_3)_3]^+$, m/z 524 $[M+H-C_{16}H_{29}CH=C=O]^+$, m/z 506 $[524-H_2O]^+$, m/z
47 502 $[M+H-C_{16}H_{33}CH=C=O-H_2O]^+$ and m/z 341 $[M-HPO_4CH_2CH_2N(CH_3)_3-C_{16}H_{29}CHC=O]^+$ were
48 detected (see **Fig. 6a** and **Fig. 7a**). In the fragmentation of standard PS (16:0/18:1), the
49 characteristic daughter ions at m/z 577 $[M+H-185]^+$ derived from molecular ion at m/z 762
50 $[M+H]^+$ by losing the phosphate head group.²¹ Simultaneously, the other daughter ions at m/z 239
51 $[C_{15}H_{29}C=O]^+$, m/z 265 $[C_{17}H_{33}C=O]^+$, m/z 313 $[M+H-C_{16}H_{32}CH=C=O]^+$ and m/z 339
52 $[M+H-C_{14}H_{28}CHC=O]^+$ were detected (see **Fig. 8a** and **Fig. 9a**).
53
54
55
56
57
58
59
60

In ESI (-) mode, the characteristic ions at m/z 168 [$C_4H_{11}O_4NP$]⁻ and m/z 673 [$M-H-87$]⁻ of PC (18:0/18:2) and PS (16:0/18:1) were found respectively, besides other daughter ions of them (see **Fig. 7b** and **Fig. 9b**).^{21,33,34} Differently with PE and PI, the abundance ratios of the *sn*-1/*sn*-2 carboxylate anions of PC and PS were not changed, the ratio of the *sn*-1/*sn*-2 carboxylate anions of PC was less than 1 at collision energies of 20-50 eV (see **Fig. 6b**), while the ratio of PS was more than 1 at collision energies of 20-50 eV (see **Fig. 8b**). As shown in **Fig. 5**, PC preferred to form five-membered ring and produced the higher intensity of ions at m/z 279 [R_2COO]⁻, which was considered that the steric hindrance of substituent group of phosphate head group hindered the assault of anionic site of phosphate group at C-1 of glycerol backbone. PS intended to form the six-membered ring transition state and acquired the higher intensity of ions at m/z 255 [R_1COO]⁻. Summing up the above, the abundance ratio of the *sn*-1/*sn*-2 carboxylate anions could provide useful information of the positions of the two acyl chains.

Fig. 6

Fig. 7

Fig. 8

Fig. 9

3.3 The fragmentation regularity of SM

SM, different with glycerophospholipids in chemical structure, is consisted of a sphingosine, an acyl chain and choline. The fragmentation patterns in different ion modes were shown in **Fig. 10**. In ESI (+) mode, SM (d18:1/18:0) could formed the molecular ion at m/z 731 [$M+H$]⁺ and characteristic ion at m/z 184 [$C_5H_{15}O_4NP$]⁺. The other daughter ions at m/z 713 [$731-H_2O$]⁺, 447 [$713-C_{16}H_{33}CH=C=O$]⁺, 654 [$713-(CH_3)_3N$]⁺, and 530 [$713-HPO_4CH_2CH_2N(CH_3)_3$]⁺ could be detected. In ESI (-) mode, it was easy for SM (d18:1/18:0) to produce ions at m/z 715 [$M-CH_3$]⁻ and adduct molecular ions at m/z 789 [$M+CH_3COO$]⁻ when the mobile phase contained acetic acid (shown in **Fig. 11**). Similar to PC, SM has the same characteristic ion at m/z 168 [$C_4H_{11}O_4NP$]⁻ when the collision energies exceed 30 eV (**Fig. 10**). It was worth noting that PC and SM with the similar structure of polar head group were difficult to be distinguished only by characteristic daughter ions in ESI (+) or ESI (-) mode. It was found that PC has the *sn*-1 and *sn*-2 carboxylate anions with different relative abundance in ESI (-) mode while SM has not (**Fig. 10b**), which could be used to distinguish SM and PC.

Fig. 10

Fig. 11

3.4 Regular ion patterns of phospholipid standards from MS

The regular ion patterns of five phospholipid standards and their abundance ratios of the *sn*-1/*sn*-2 carboxylate anions in different ion modes were studied through analysis of the MS/MS information. As shown in **Table 1**, different phospholipids can produce characteristic ions and neutral loss associated with fragmentation reactions of their specific polar head groups. The PE produced the unique daughter ions $[C_2H_7O_4NP]^-$ at m/z 140 and $[C_5H_{11}O_5NP]^-$ at m/z 196 in ESI (-) mode, and the daughter ions $[M+H-141]^+$ due to the neutral loss of $C_2H_8O_4NP$ (141 Da) in ESI (+) mode. The characteristic ions $[C_6H_{10}O_8P]^-$ at m/z 241 of PI were detected in ESI (-) mode. PC and SM with same structure of phosphate head groups could produce the daughter ions at m/z 184 $[C_5H_{15}O_4NP]^+$ in ESI (+) mode and m/z 168 $[C_4H_{11}O_4NP]^-$ in ESI (-) mode. In addition, the molecular ion $[M-H]^-$ of PS could produce the ion $[M-H-87]^-$ as a result of neutral loss of its head group $C_3H_5O_2N$ (87 Da). Furthermore, the nonspecific ions $[C_3H_6O_5P]^-$ (m/z 153) were also found, a common fragment formed by all glycerol-phospholipids in ESI (-) mode. It was observed that these specific head group fragmentations allowed the specific detection of different phospholipid classes.

3.5 Different patterns of fatty acyl chains of glycerophospholipids

In this work, the different patterns of fatty acyl chains of phospholipids were researched. For examples, C20:4 of PE (18:0/20:4) and PI (18:0/20:4) have patterns of $C_{18}H_{33}CH=C=O$ and ion at m/z 303 $[R_2COO]^-$, and C16:0 of PS (16:0/18:1) have patterns of ions at m/z 255 $[R_1COO]^-$ and m/z 239 $[C_{15}H_{29}C=O]^+$. Summarizing these five phospholipids and our previous results,^{22,23} the fatty acyl chains of glycerophospholipids have three patterns of $[RC=O]^+$ in ESI (+) mode, $[RCOO]^-$ in ESI (-) mode, and neutral ion $R'CH=CO$ in all ion modes. Among them, the R was the long carbon chains and the R' represented the carbon chains which was less 14 Da ($-CH_2-$) than R. The fragment patterns and formula weight of common fatty acyl chains contributed to fast identify the type of fatty acyl chains of phospholipids by the fragment ions detected in ESI modes were list in **Table 2**. Additionally, the ratios of the *sn*-1/*sn*-2 carboxylate anions in different collision energies used to confirm the positions of carboxylate anions were summarized in **Table 1**.

Table 2

4 Conclusions

In this paper, the fragmentation regularities of the five types of phospholipids were studied systematically in different ion modes. Combining with our previous work,^{22,23} all these fragmentation regularities were summarized, containing three patterns ($[\text{RC}=\text{O}]^+$, $[\text{RCOO}^-]$ and $\text{R}'\text{CH}=\text{CO}$) of common fatty acyl chain ions in different ion modes, the variation trend of ratios of the *sn*-1/*sn*-2 carboxylate anions, and different characteristic ions at different collision energies (10-50 eV). These proposed methodologies have already been successfully applied to identify high-throughput screening of phospholipids markers in phospholipidomics studies.¹²⁻¹⁴ These facts have proved that quick and effective data mining is more and more necessary especially with increasingly abundant information and increasingly growing database in nowadays. The results observed in this paper provide the reference tools for rapid identification of phospholipids and the opportunity to obtain complementary and more comprehensive data in future phospholipidomics studies, which help minimize or even avoid the risk of lipid loss and misidentification. Although many of the presented observations have been already reported for similar ionization techniques,^{20,21,35} it is infrequent that such complex information is presented within a single publication base a lot of experimental application foundation,^{22,23} simultaneously covering five lipid categories analyzed in both polarity modes by the use of ESI-Q-TOF-MS. It will complete identification by checking our tables and figures. In addition, researchers can list more fatty acyl chain fragmentation ions seldom-used but suit their research needs according to the rules of Table 2.

Acknowledgements

This work was supported by National Science Foundation Project in Guangdong Province (Grant No. 21275036), P. R. China.

References

- 1 H. Hirschmann, *J. Biol. Chem.* 1960, 235, 2762.
- 2 A. A. Farooqui and L. A. Horrocks, *Neuroscientist*, 2001, 7, 232.
- 3 M-J. Lee, J. R. Van Brocklyn, S. Thangada, C. H. Liu, A. R. Hand, R. Menzeleev, S. Spiegel and T. Hla, *Science*, 1998, 279, 1552.
- 4 G. Di Paolo, H. S. Moskowitz, K. Gipson, M. R. Wenk, S. Voronov, M. Obayashi, R. Flavell, R. M. Fitzsimonds, T. A. Ryan and P. De Camilli, *Nature*, 2004, 431, 415.
- 5 Y. Takuwa, H. Okamoto, N. Takuwa, K. Gonda, N. Sugimoto and S. Sakurada, *Mol. Cell. Endocrinol*, 2001, 177, 3.
- 6 P. Mattjus, B. Malewicz, J. T. Valiyaveetil, W. J. Baumann, R. Bittman and R. E. Brown, *J.*

- 1
2
3
4 *Biol. Chem.*, 2002, 277, 19476.
- 5
6
7
8
9
10
11
12
13
14
15
16
17
18
19
20
21
22
23
24
25
26
27
28
29
30
31
32
33
34
35
36
37
38
39
40
41
42
43
44
45
46
47
48
49
50
51
52
53
54
55
56
57
58
59
60
- 7 D. A. Brown and E. London, *J. Biol. Chem.*, 2000, 275, 17221.
- 8 A. M. Hodge, D. R. English, K. O' Dea, A. J. Sinclair, M. Makrides, R. A. Gibson and G. G. Giles, *Am. J. Clin. Nutr.*, 2007, 86, 189.
- 9 X. Han, D. R. Abendschein, J. G. Kelley and R. W. Gross, *Biochem. J.*, 2000, 352, 79.
- 10 N. Attia, N. Domingo, A. M. Lorec, A. Nakbi, S. Hammami, K. Ben Hamda, H. Portugal, D. Lairon, M. Hammami and F. Chanussot, *Clin. Biochem.*, 2009, 42, 845.
- 11 R. de Vries, P. J. W. H. Kappelle, G. M. Dallinga-Thie and R. P. F. Dullaart, *Atherosclerosis*, 2011, 217, 253.
- 12 L. Liu, M. Wang, X. Yang, M. Bi, L. Na, Y. Niu, Y. Li and C. Sun, *Clin. Chem.*, 2013, 59, 1388.
- 13 A. Floegel, N. Stefan, Z. H. Yu, K. Mühlenbruch, D. Drogan, H. G. Joost, A. Fritsche, H. U. Häring, M. Hrabě de Angelis, A. Peters, M. Roden, C. Prehn, R. Wang-Sattler, T. Illig, M. B. Schulze, J. Adamski, H. Boeing and T. Pischon, *Diabetes*, 2013, 62, 639.
- 14 C. Zhu, Q. L. Liang, P. Hu, Y. M. Wang and G. A. Luo, *Talanta*, 2011, 85, 1711.
- 15 K. Yokoyama, F. Shimizu and M. Setaka, *J. Lipid Res.*, 2000, 41, 142.
- 16 T. Sano, D. Baker, T. Virag, A. Wada, Y. Yatomi, T. Kobayashi, Y. Igarashi and G. Tigyí, *J. Biol. Chem.*, 2002, 277, 21197.
- 17 A. R. Nor Aliza, J. C. Bedick, R. L. Rana, H. Tunaz, W. W. Hoback and D. W. Stanley, *Comp. Biolchem. Phys. A Mol. Integr. Physiol.*, 2001, 128, 251.
- 18 K. Y. Tserng and R. Griffin, *Anal. Biochem.* 2003, 323, 84.
- 19 M. Farré, M. Gros, B. Hernández, M. Petrovic, P. Hancock and D. Barceló, *Rapid Commun. Mass Spectrom.*, 2008, 22, 41.
- 20 E. Hvattum, G. Hagelin and A. Larsen. *Rapid Commun. Mass Spectrom.*, 1998, 12, 1405.
- 21 X. J. Yan, H. Y. Li, J. L. Xu and C. X. Zhou, *Chin. J. Oceanol. Limnol.*, 2010, 28, 106.
- 22 J. J. Pi, X. Wu, S. T. Yang, P. Y. Zeng and Y. F. Feng, *J. Sep. Sci.*, 2015, 38, 886.
- 23 Y. Q. She, J. A. Song, E. Yang, L. L. Zhao, Y. M. Zhong, W. Rui, Y. F. Feng and X. Wu, *Biomed. Chromatogr.*, 2014, 28, 1744.
- 24 J. F. Brouwers, E. A. Vernooij, A. G. Tielens and L. M. Van Golde, *J. Lipid Res.*, 1999, 40, 164.

- 1
2
3
4
5
6
7
8
9
10
11
12
13
14
15
16
17
18
19
20
21
22
23
24
25
26
27
28
29
30
31
32
33
34
35
36
37
38
39
40
41
42
43
44
45
46
47
48
49
50
51
52
53
54
55
56
57
58
59
60
- 25 E. A. Vernooij, J. F. Brouwers, J. J. Kettenes-Van den Bosch and D. J. Crommelin, *J. Sep. Sci.*, 2002, 25, 285.
- 26 R. Taguchi, J. Hayakawa, Y. Takeuchi and M. Ishida, *J. Mass Spectrom.*, 2000, 35, 953.
- 27 J. A. Zirrolli, K. L. Clay and R. C. Murphy, *Lipids*, 1991, 26, 1112.
- 28 H. Münster and H. Budzikiewicz, *Biol. Chem. Hoppe-Seyler*, 1988, 369, 303.
- 29 R. N. A. H. Lewis and R. N. McElhaney, *Chem. Phys. Lipids*, 1998, 96, 9.
- 30 J. L. Kerwin, A. R. Tuininga and L. H. Ericsson, *J. Lipid Res.*, 1994, 35, 1102.
- 31 P. E. Haroldsen and S. J. Gaskell, *Biomed. Environ. Mass Spectrom.*, 1989, 18, 439.
- 32 D. Zhang, X. Chen, Z. Song, X. Yu, T. Zhang and K. Bi, *Zhongnan Yaoxue*, 2010, 8, 593.
- 33 K. A. Harrison and R. C. Murphy, *J. Mass Spectrom.*, 1995, 30, 1772.
- 34 Y. P. Ho and P. C. Huang, *Rapid Commun. Mass Spectrom.* 2002, 16, 1582.
- 35 J. Godzien, M. Ciborowski, M. P. Martínez-Alcazar, P. Samczuk, A. Kretowski and C. Barbas, *J. Proteome Res.*, 2015, 14, 3204.

Table 1 Characteristic ions and neutral loss of different phospholipids in ESI modes

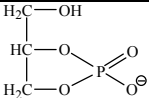
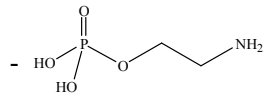
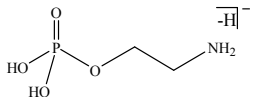
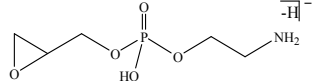
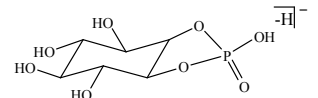
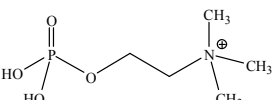
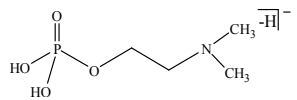
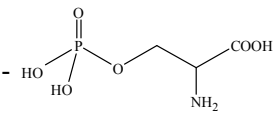
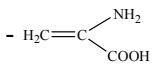
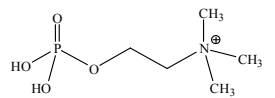
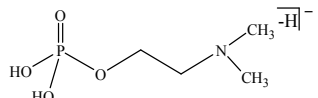
Type	ESI (+)		ESI (-)		<i>sn</i> -1/ <i>sn</i> -2, (Collision Energy, eV)
	Fragment structure	<i>m/z</i>	Fragment structure	<i>m/z</i>	
All glycerophospholipids				153	
PE		[M+H-141] ⁺		140	<1, (20-30 eV) >1, (40-50 eV)
				196	
PI				241	<1, (20-30 eV) >1, (40-50 eV)
PC		184		168	<1, (20-50 eV)
PS		[M+H-185] ⁺		[M-H-87] ⁻	>1, (20-50 eV)
SM		184		168	

Table 2 Possible ions of the common fatty acyl chains of phospholipids in ESI modes

Type	ESI(+) [RC=O] ⁺ (<i>m/z</i>)	ESI(-) [RCOO] ⁻ (<i>m/z</i>)	ESI(+/-) R'CH=CO (natural loss)	Type	ESI(+) [RC=O] ⁺ (<i>m/z</i>)	ESI(-) [RCOO] ⁻ (<i>m/z</i>)	ESI(+/-) R'CH=CO (natural loss)
C12:0	183	199	182	C18:2	263	279	262
C14:0	211	227	210	C20:1	293	309	292
C15:0	225	241	224	C20:3	289	305	288
C16:0	239	255	238	C20:4	287	303	286
C16:1	237	253	236	C20:5	285	301	284
C17:1	251	267	250	C22:1	321	337	320
C18:0	267	283	266	C22:5	313	329	312
C18:1	265	281	264	C22:6	311	327	310

1
2
3
4
5
6
7
8
9
10
11
12
13
14
15
16
17
18
19
20
21
22
23
24
25
26
27
28
29
30
31
32
33
34
35
36
37
38
39
40
41
42
43
44
45
46
47
48
49
50
51
52
53
54
55
56
57
58
59
60

Figure captions

Fig. 1 MS/MS spectra of PE (18:0/20:4) in ESI (+) (a) and ESI (-) (b) modes at different collision energies (10 eV, 20 eV, 30 eV, 40 eV, 50 eV)

Fig. 2 The fragmentation pathways of PE (18:0/20:4) in ESI (+) (a) and ESI (-) (b) modes

Fig. 3 MS/MS spectra of PI (18:0/20:4) in ESI (+) (a) and ESI (-) (b) modes at different collision energies (10 eV, 20 eV, 30 eV, 40 eV, 50 eV)

Fig. 4 The fragmentation pathways of PI (18:0/20:4) in ESI (+) (a) and ESI (-) (b) modes

Fig. 5 Mechanism leading to the formation of *sn*-1 and *sn*-2 carboxylate ions from glyceryl phospholipids in ESI (-) mass spectrometry (adapted from Vernooij²⁵)

Fig. 6 MS/MS spectra of PC (18:0/18:2) in ESI (+) (a) and ESI (-) (b) modes at different collision energies (10 eV, 20 eV, 30 eV, 40 eV, 50 eV)

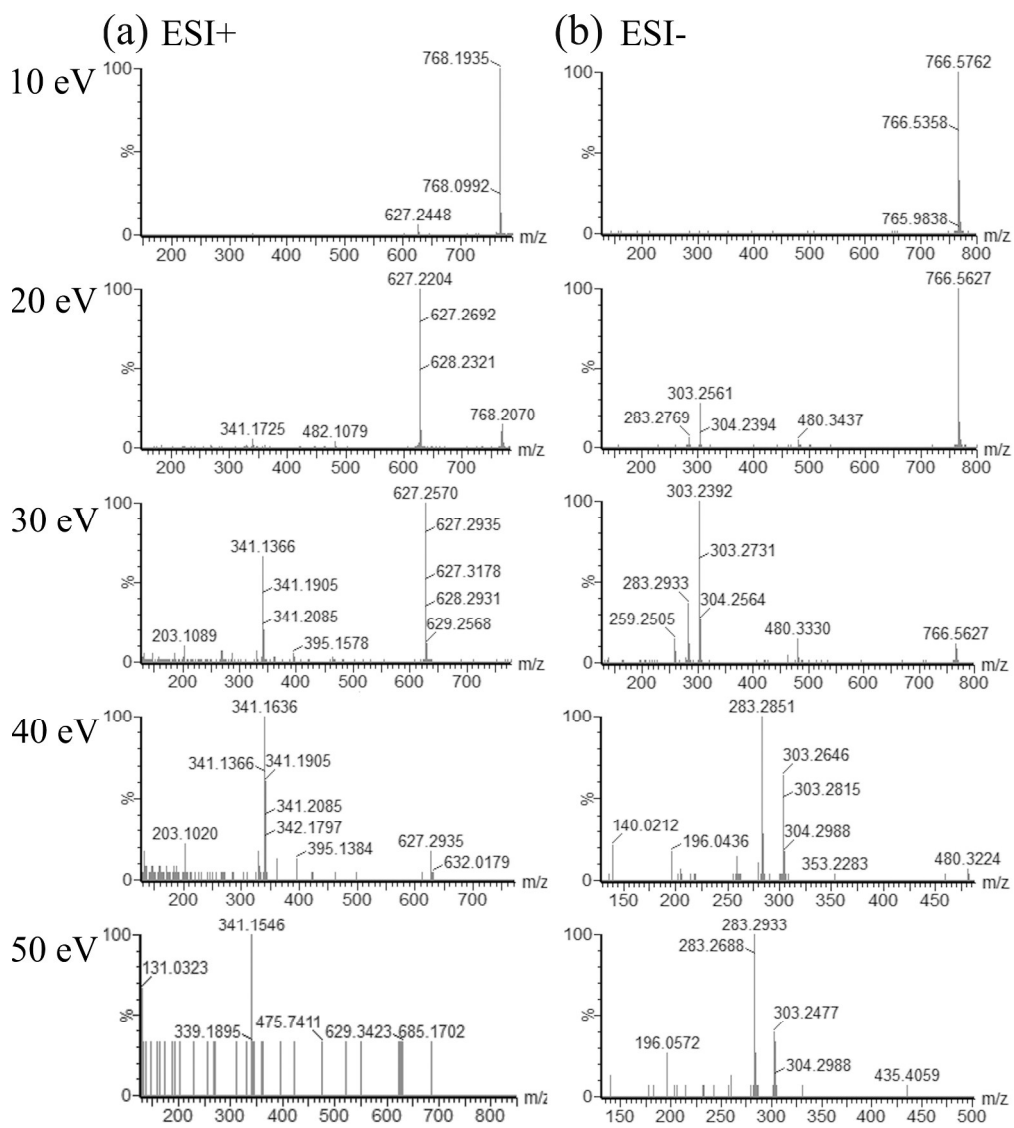
Fig. 7 The fragmentation pathways of PC (18:0/18:2) in ESI (+) (a) and ESI (-) (b) modes

Fig. 8 MS/MS spectra of PS (16:0/18:1) in ESI (+) (a) and ESI (-) (b) modes at different collision energies (10 eV, 20 eV, 30 eV, 40 eV, 50 eV)

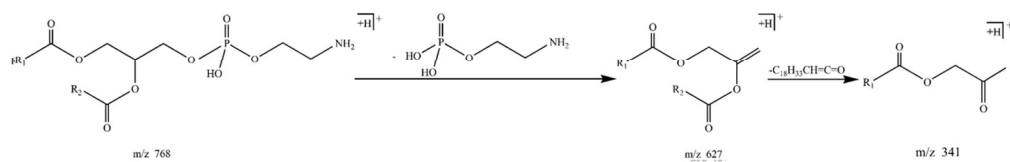
Fig. 9 The fragmentation pathways of PS (16:0/18:1) in ESI (+) (a) and ESI (-) (b) modes

Fig. 10 MS/MS spectra of SM (d18:1/18:0) in ESI (+) (a) and ESI (-) (b) modes at different collision energies (10 eV, 20 eV, 30 eV, 40 eV, 50 eV)

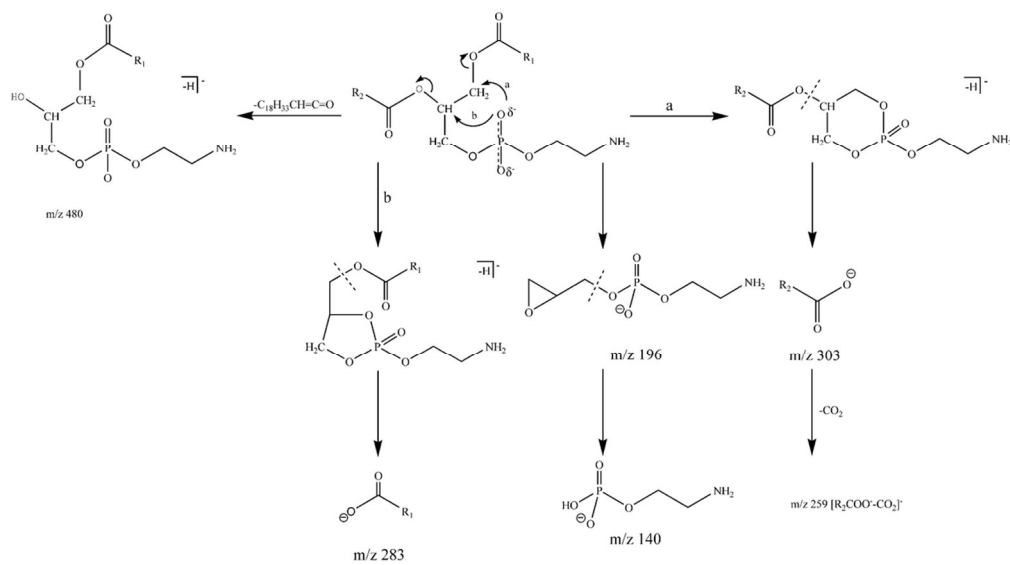
Fig. 11 The fragmentation pathways of SM (d18:1/18:0) in ESI (+) (a) and ESI (-) (b) modes



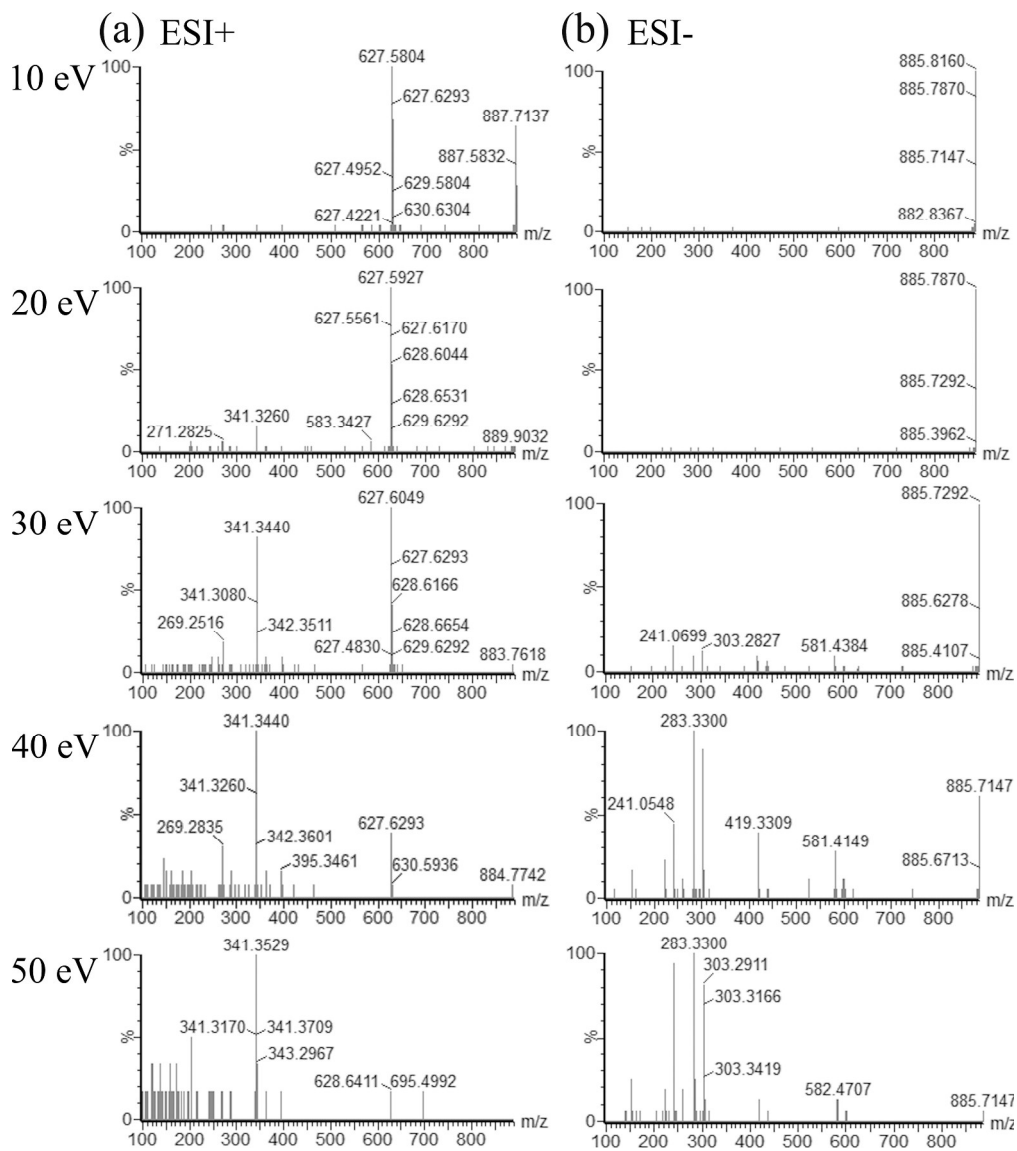
(a) ESI+



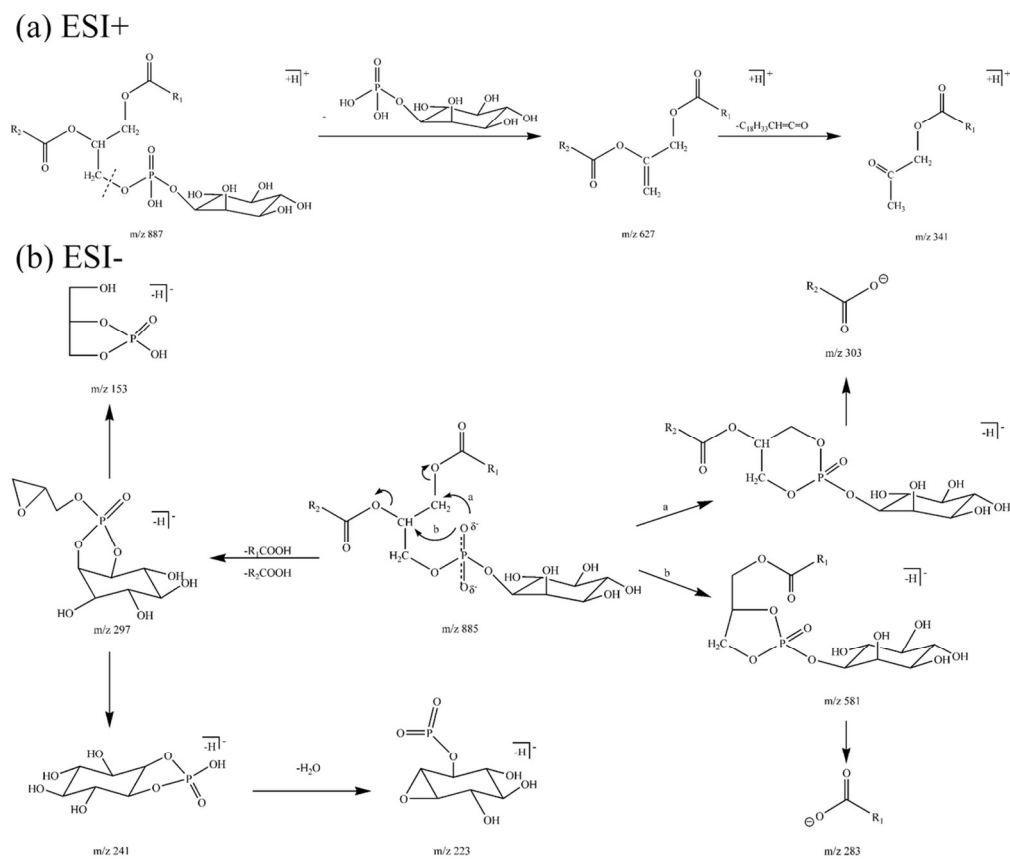
(b) ESI-

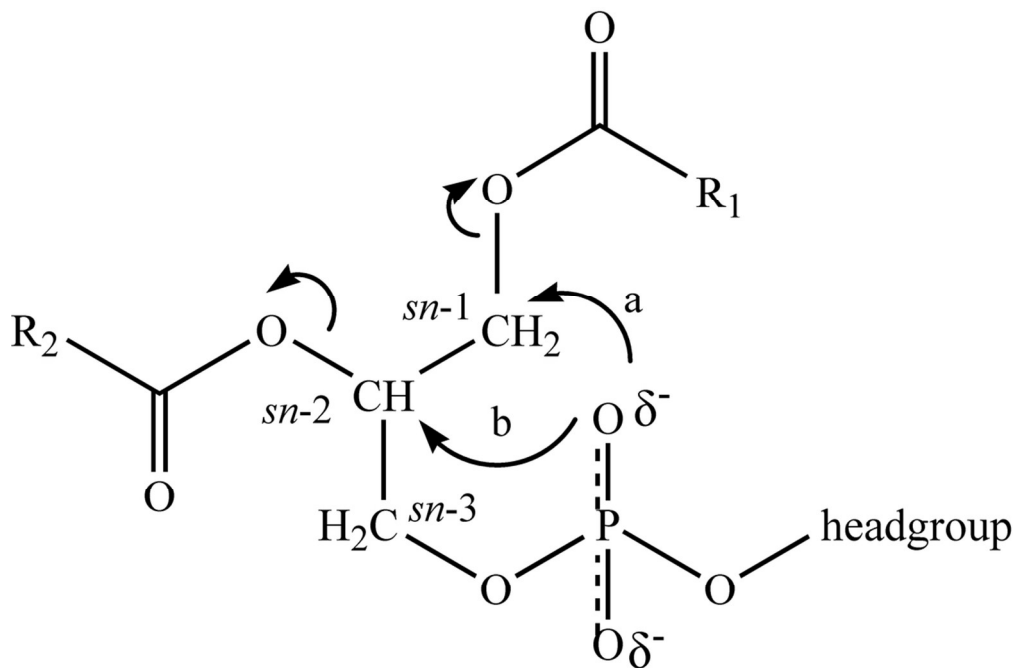


53x44mm (600 x 600 DPI)

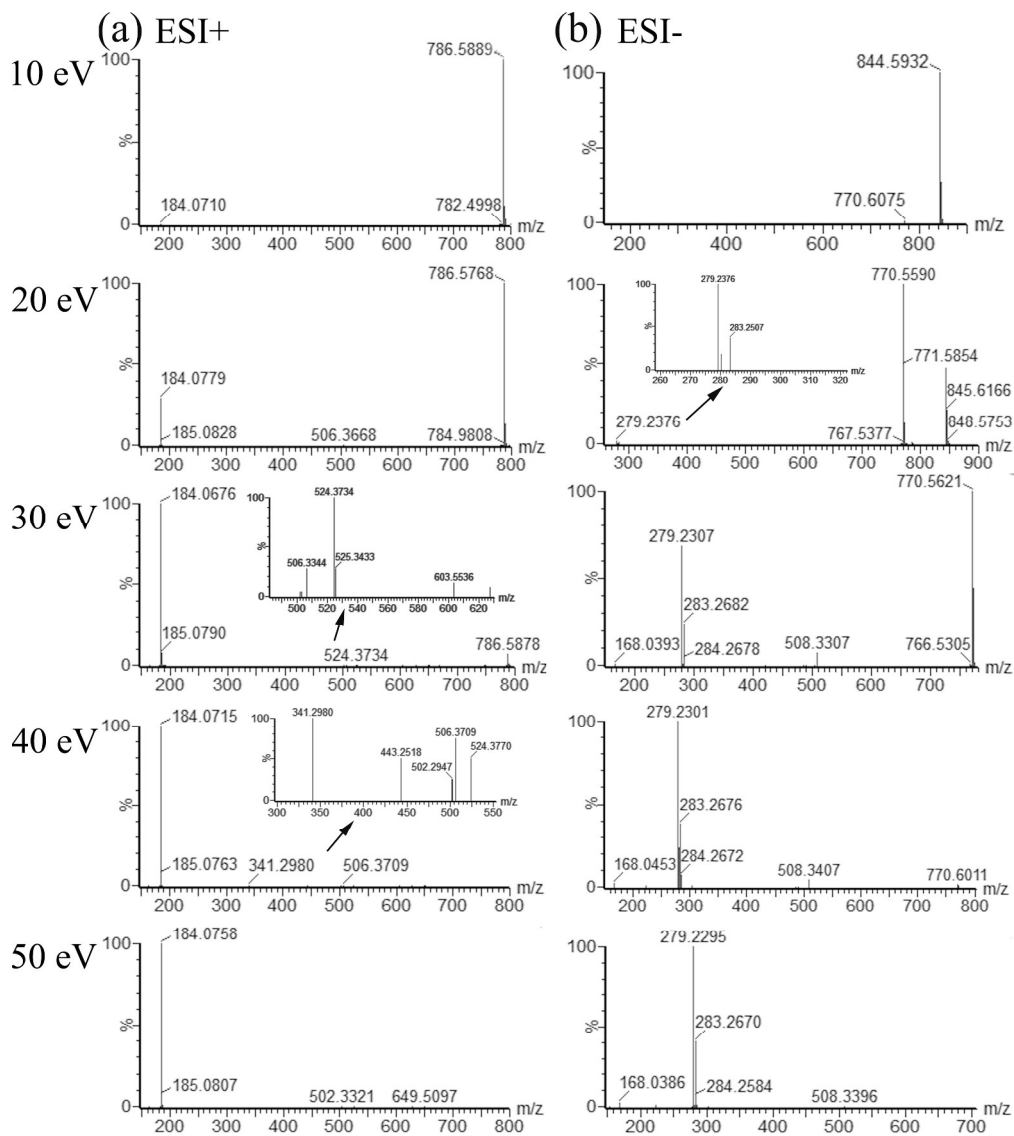


131x149mm (600 x 600 DPI)



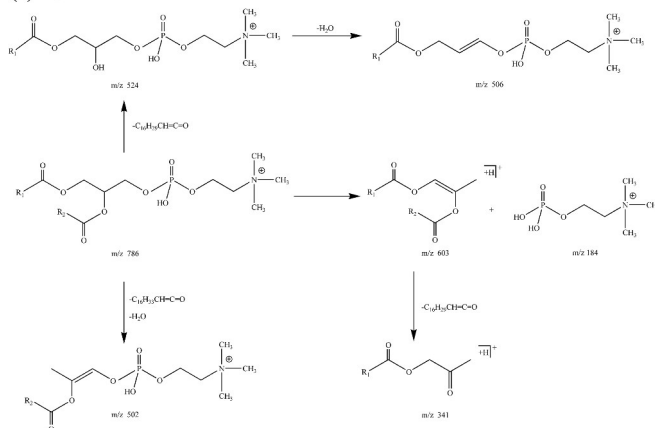


52x35mm (600 x 600 DPI)

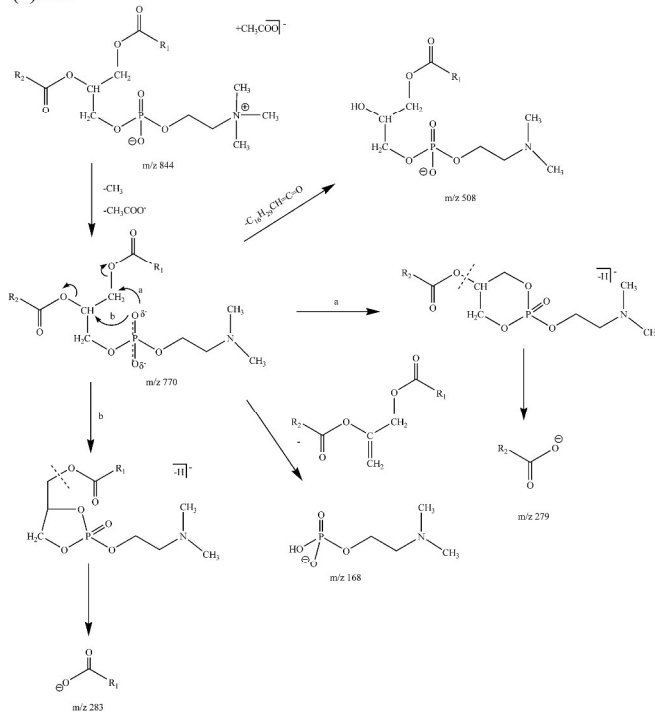


131x147mm (600 x 600 DPI)

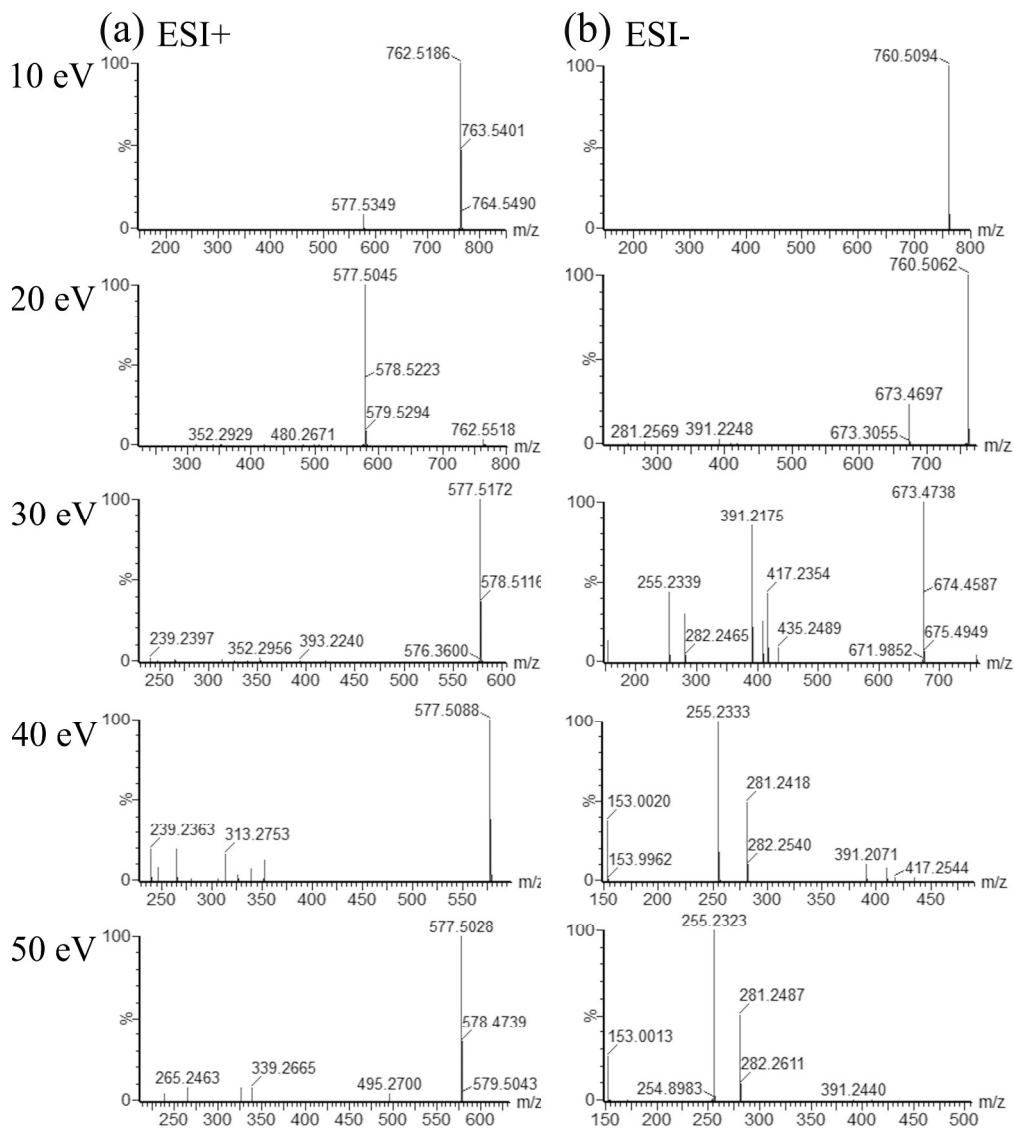
(a) ESI+



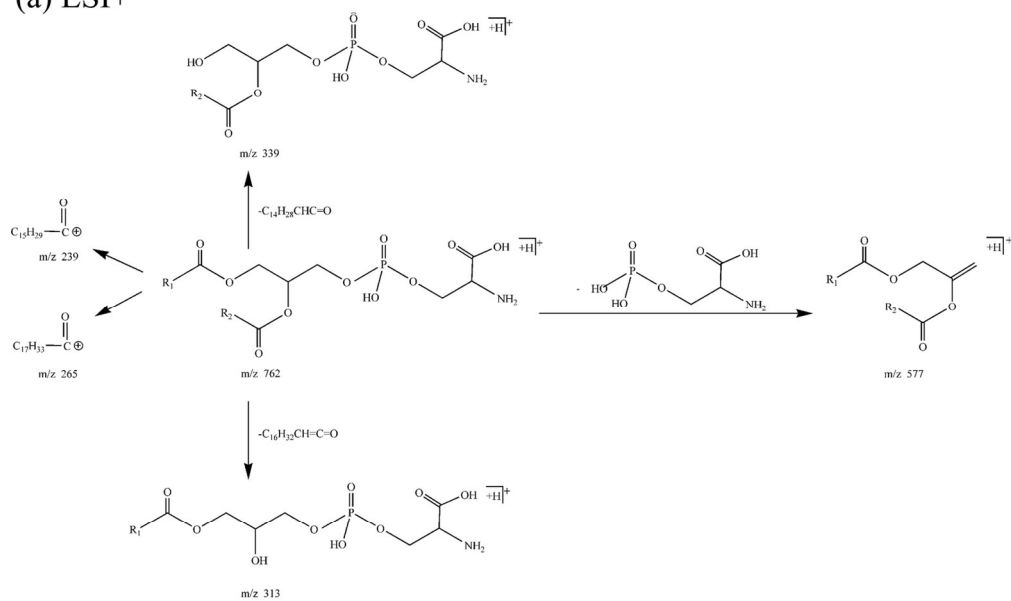
(b) ESI-



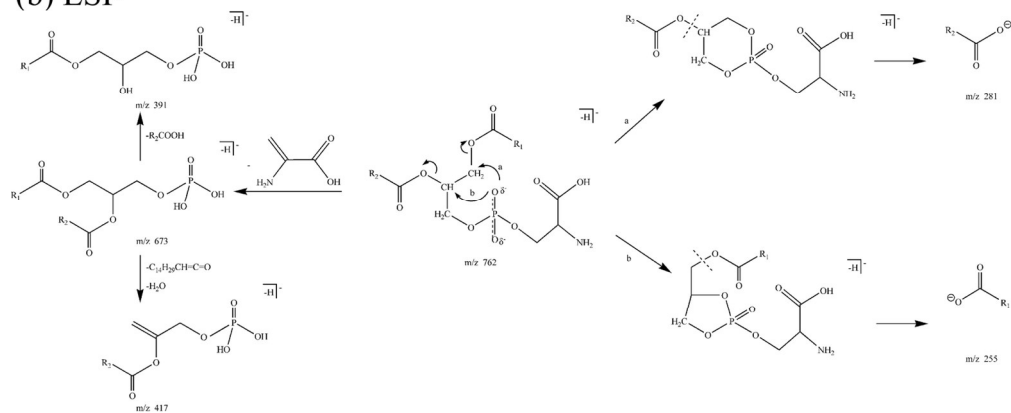
117x215mm (600 x 600 DPI)



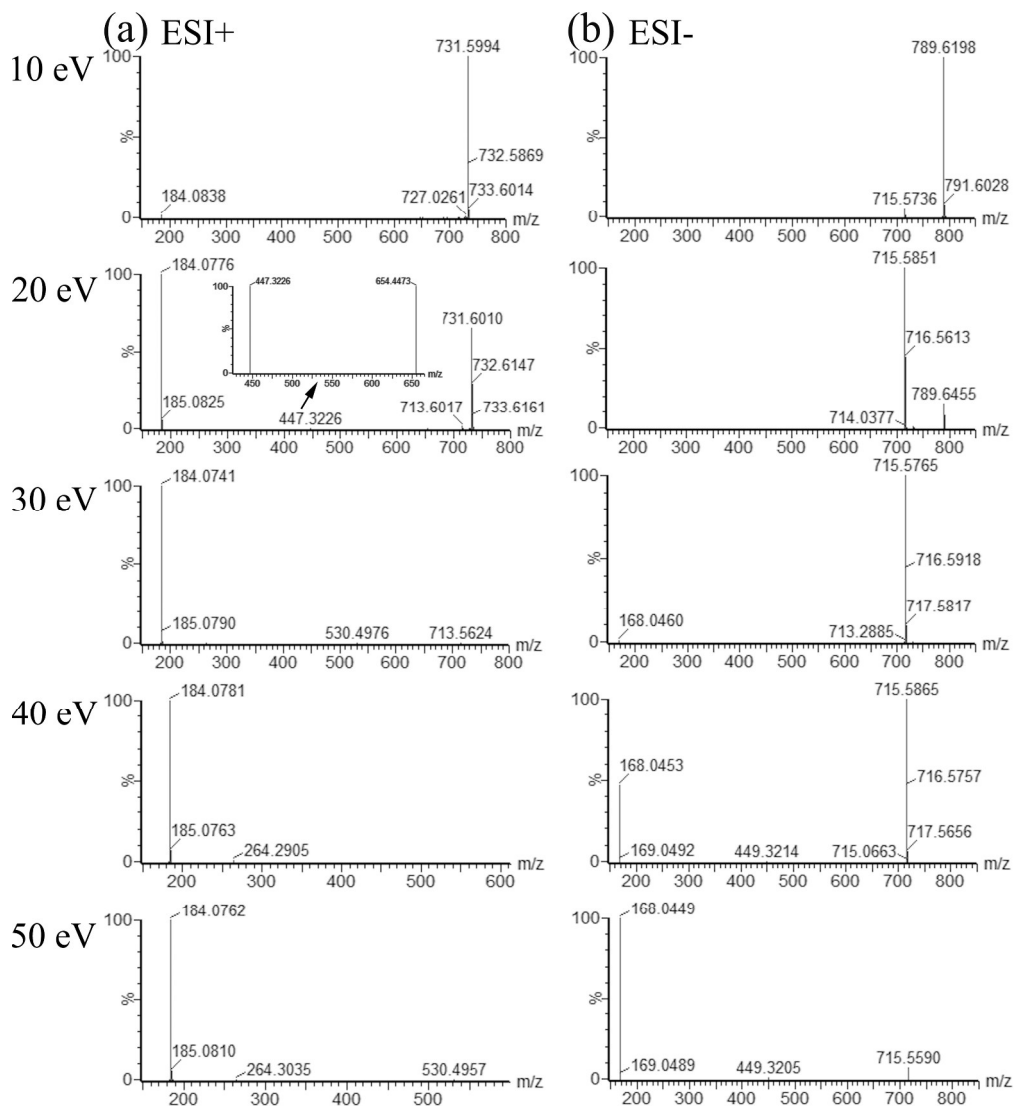
(a) ESI+



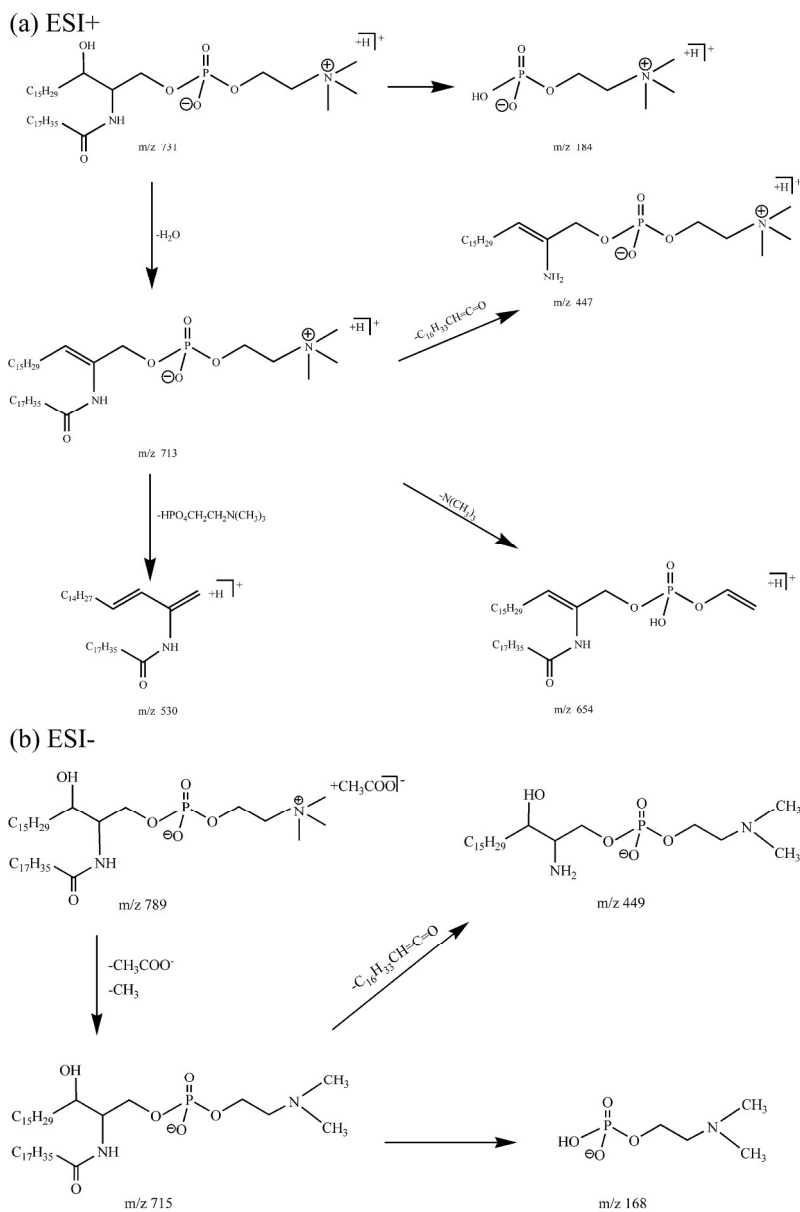
(b) ESI-



68x72mm (600 x 600 DPI)



129x141mm (600 x 600 DPI)



1
2
3
4
5
6
7
8
9
10
11
12
13
14
15
16
17
18
19
20
21
22
23
24
25
26
27
28
29
30
31
32
33
34
35
36
37
38
39
40
41
42
43
44
45
46
47
48
49
50
51
52
53
54
55
56
57
58
59
60

Fragmentation regularities of five major kinds of phospholipids including phosphatidylcholine (PC), phosphatidylethanolamine (PE), phosphatidylserine (PS), phosphatidylinositol (PI) and sphingomyelins (SM) in different ion modes at several elevated collision energies (10-50 eV) have been studied by ultra-high-performance liquid chromatography electrospray ionization quadrupole time-of-flight tandem mass spectrometry (UHPLC/ESI-Q-TOFMS). Fragmentation regularities of five major kinds of phospholipids were systematically summarized.

